

## Supporting Information

### Development of a 3D Printable and Highly Stretchable Ternary Organic-Inorganic Nanocomposite Hydrogel

Chen Hu,<sup>†</sup> Malik Salman Haider,<sup>†</sup> Lukas Hahn,<sup>†</sup> Mengshi Yang,<sup>†</sup> and Robert Luxenhofer<sup>†,§,\*</sup>

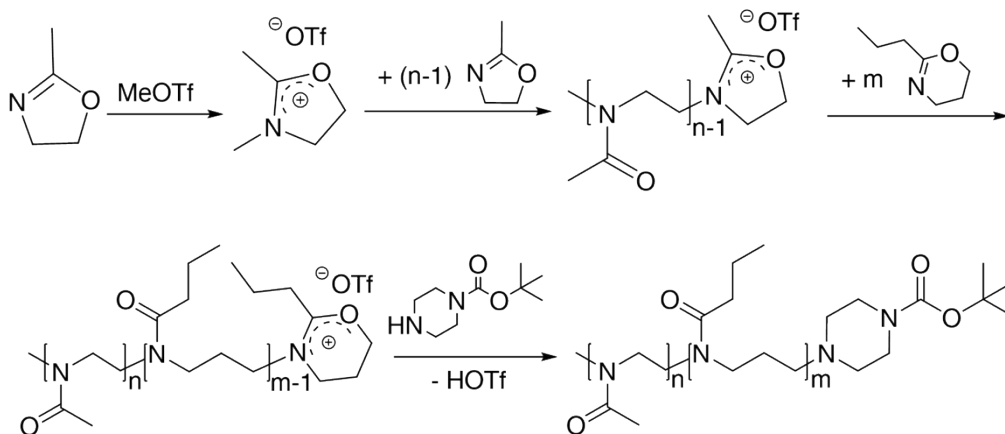
<sup>†</sup> Functional Polymer Materials, Chair for Advanced Materials Synthesis, Institute for Functional Materials and Biofabrication, Department of Chemistry and Pharmacy, Julius-Maximilians-University Würzburg, Röntgenring 11, 97070 Würzburg, Germany

<sup>§</sup> Soft Matter Chemistry, Department of Chemistry, and Helsinki Institute of Sustainability Science, Faculty of Science, University of Helsinki, 00014 Helsinki, Finland

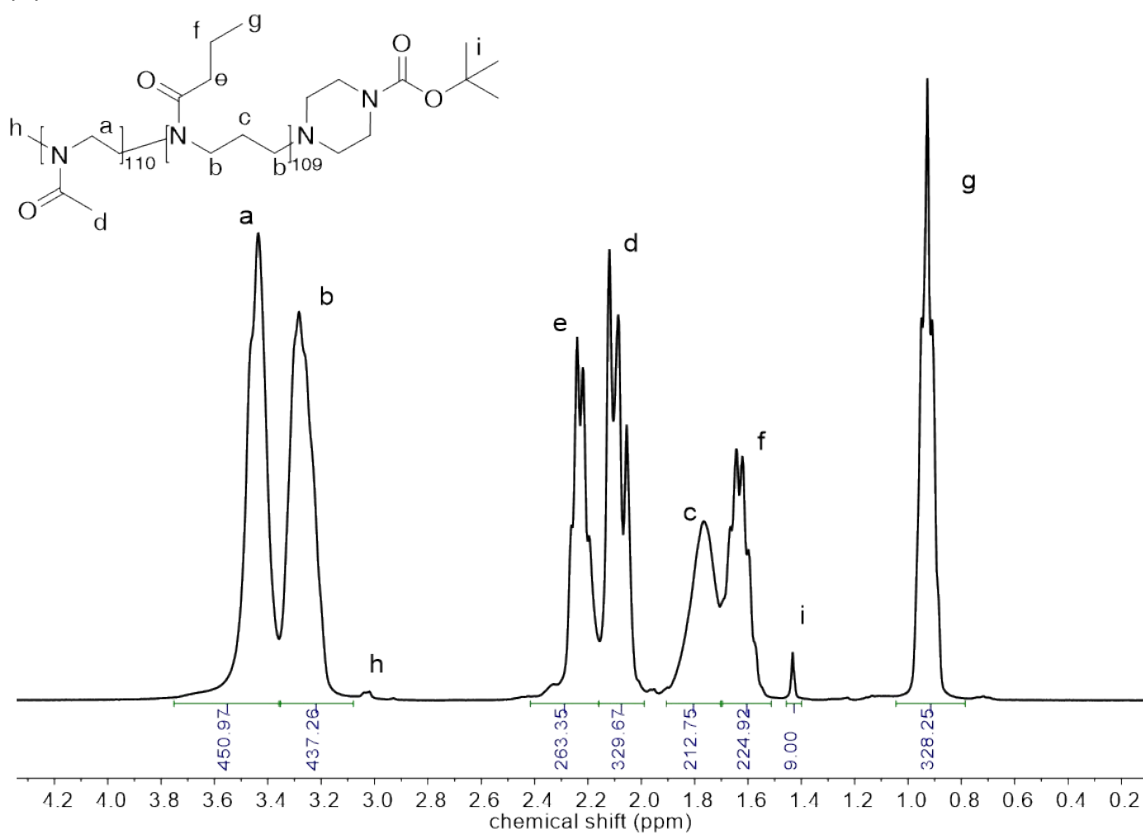
\*Corresponding author: [robert.luxenhofer@helsinki.fi](mailto:robert.luxenhofer@helsinki.fi)

### POx-*b*-POzi Polymer Synthesis and Characterization:

(a)



(b)



(c)

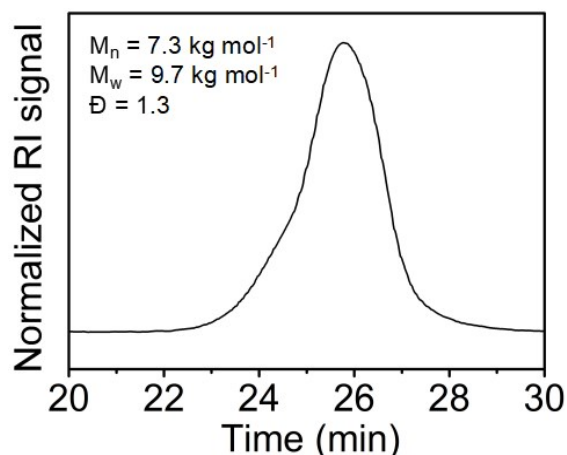


**Figure S1:** (a) Synthesis of the diblock copolymer POx-*b*-POzi *via* living cationic ring opening polymerization of 2-*n*-propyl-oxazine (nPrOzi) and 2-methyl-2-oxazoline (MeOx) monomers. Methyl triflate (MeOTf) was used as initiator and 1-Boc-piperazine as terminating agent; (b) <sup>1</sup>H-NMR of lyophilized diblock copolymer POx-*b*-POzi (CDCl<sub>3</sub>). From the signals in the <sup>1</sup>H NMR spectrum with chemical shifts at 2.09 ppm (CH<sub>3</sub> of PMeOx) and 0.93 ppm (CH<sub>3</sub> of PnPrOzi), the relative block lengths and diblock copolymer composition was determined to be POx<sub>110</sub>-*b*-POzi<sub>109</sub>. (c) GPC profile of the diblock copolymer.

#### Optimization details of the hydrogel precursor solution composition in the view of rheology and mechanical strength:

**Table S1:** Screening experiments for optimizing the system composition in view of rheological property and mechanical strength.

Composition <sup>a</sup>	POx- <i>b</i> -POzi (g)	DMAA (g)	MBAA/KPS <sup>b</sup> (g)	Water (g)	2 wt% clay solution (g)
30:10:0	1.2	0.4	0.002	2.4	/
<b>30:10:1.2</b>	<b>1.2</b>	<b>0.4</b>	<b>0.002</b>	<b>/</b>	<b>2.4</b>
30:15:0	1.2	0.6	0.003	2.2	/
30:15:1.2	1.2	0.6	0.003	/	2.2

<sup>a</sup> The composition is labeled by x: y: z, where x is the mass fraction of copolymer POx-*b*-POzi, y is the mass fraction of monomer DMAA, z means the mass fraction of clay. <sup>b</sup> The cross linker MBAA (N, N'-Methylenebisacrylamide) and initiator KPS (Potassium persulfate) are both 0.5 wt% of DMAA. "/" means not included.

**Table S2:** Screening experiments for the amount of cross linker MBAA.

No.	POx- <i>b</i> -POzi (g)	DMAA (g)	MBAA (g)	KPS (g)	2 wt% clay solution (g)
1	1.2	0.4	0.0004	0.002	2.4
2	1.2	0.4	0.0020	0.002	2.4
3	1.2	0.4	0.0040	0.002	2.4

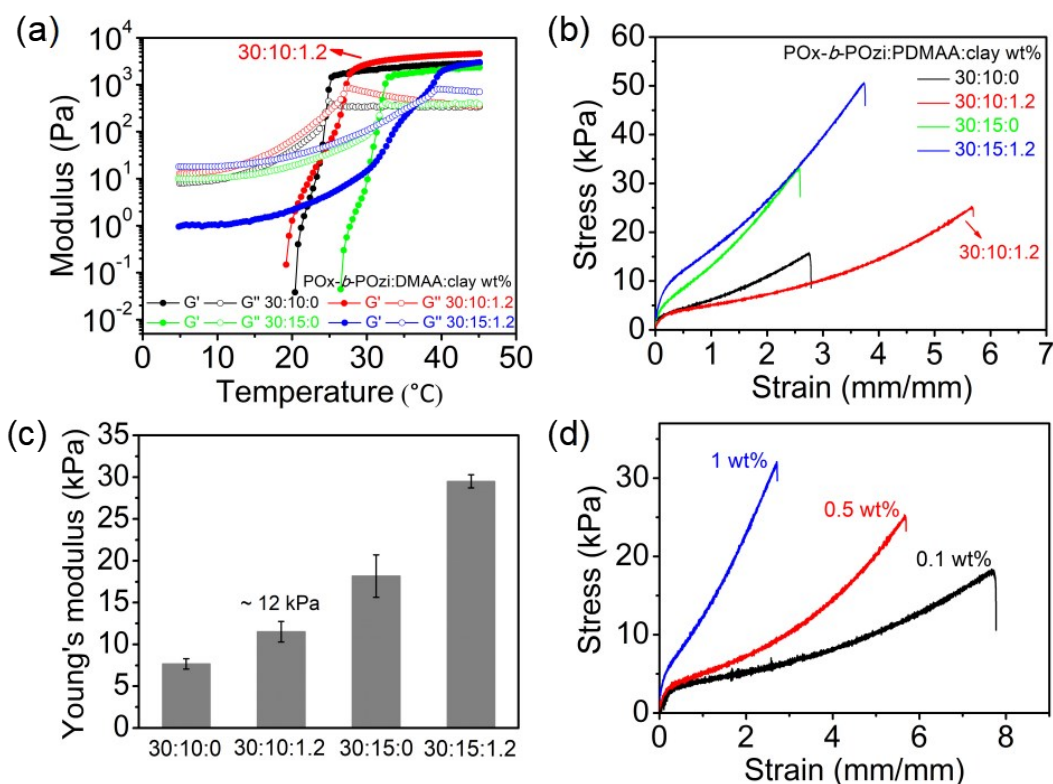


**Figure S2:** Screening experiments for optimizing the hydrogel composition in view of rheological property and mechanical strength. (a) Temperature dependent rheological measurements to investigate the thermogelling property of different compositions. (b) Tensile stress-strain curves of different compositions. (c) The corresponding Young's modulus of different compositions obtained from the tensile stress-strain curves. (d) Investigated the effects of chemical cross-linker MBAA amount on the mechanical properties of POx-*b*-POzi/PDMAA/clay hydrogel (30:10:1.2).

A relatively sharp gel transition at room to physiological temperature ( $T_{\text{gel}}$ ) will lead to the rapid gelation under a mild condition conveniently, and this together with a relatively higher storage modulus ( $G'$ ) of the gel formed will facilitate the instant shape

maintenance of the print structure. As the thermogelation hinges on thermoreversible hydrophobic interactions, the addition of significant amounts of DMAA could affect the thermogelation (Figure S2a). Indeed, when 15 wt.% DMAA were added, the gelation temperature increased significantly, i.e., the thermogelation property was weakened. In contrast, at 10 wt.% DMAA, the effect was minor. And the sample of composition 30:10:1.2 showed a desired combination of  $T_{gel}$  around 27 °C and  $G'$  over 4.5 kPa. Additionally, their mechanical properties after chemical curing were also investigated to understand the hydrogel strength and elongation of different compositions (Figure S2b, c). Although increasing the amount of monomer DMAA will enhance the mechanical strength of the hydrogel, it will over-compromise the thermogelling property of the hydrogel system, and result in poor printability. Clay addition will enhance the overall performance of the hydrogel, especially the elongation at the break. Moreover, the effects of crosslinker MBAA amount on the mechanical properties of the hydrogel was also investigated (Figure S2d). Finally, the composition (30:10:1.2) with 2 wt% clay aqueous solution as solvent, polymer concentration of 40 wt% (1:3 of DMAA/POx-*b*-POzi in weight ratio), MBAA and initiator KPS of 0.5 wt% relative to the weight of DMAA was chosen to continue the following experimental demonstration.

### The thermogelling properties of POx-*b*-POzi/AA (or HEMA)/clay hydrogels:

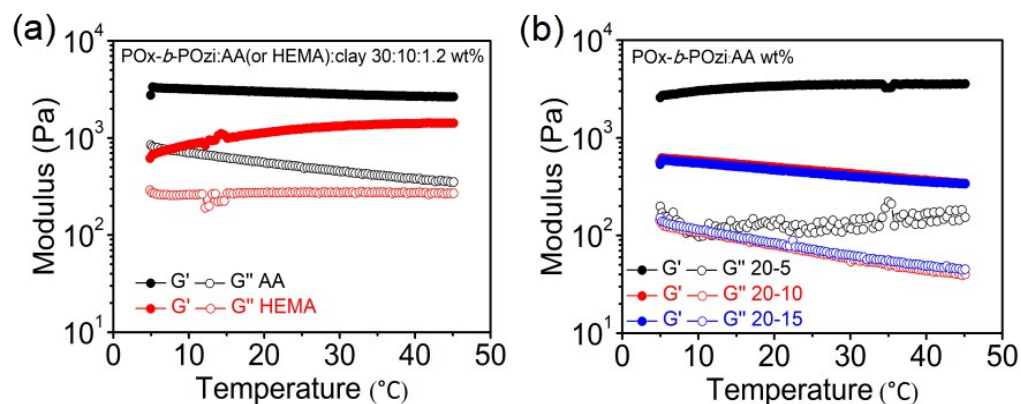


**Figure S3:** Temperature dependent rheology properties of (a) POx-*b*-POzi/AA/clay and POx-*b*-POzi/HEMA/clay system with the hydrogel composition of 30:10:1.2, and (b) POx-*b*-POzi/AA system of different compositions.

The hysteresis loops of the hydrogel at the maximum strains of 400% and 500%:

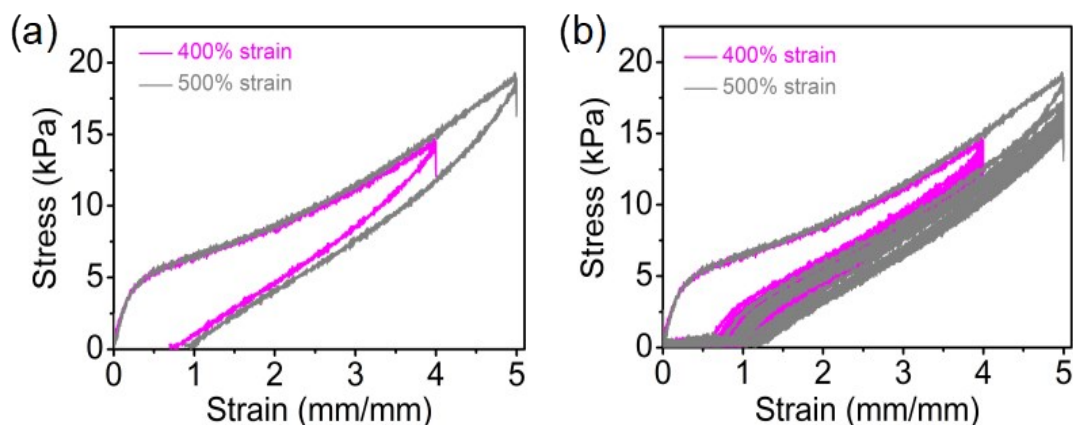


**Figure S4:** The hysteresis loops of POx-*b*-POzi/PDMAA/clay hydrogel at the maximum strains of 400% and 500%. (a) The cyclic tensile loading-unloading curves. (b) Ten immediate consecutive tensile loading-unloading curves.

Photographs of the hydrogel samples in consecutive cyclic tensile loading-unloading tests:

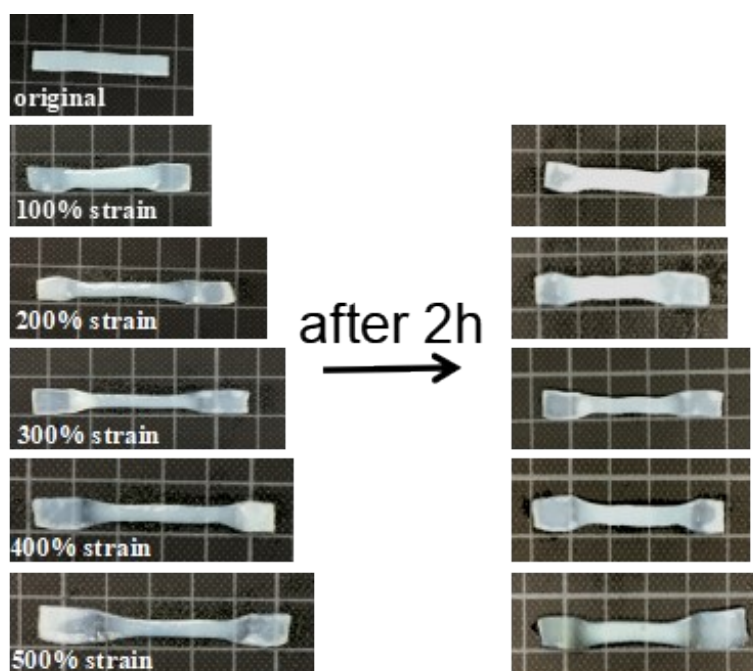


**Figure S5:** Photographs of the POx-*b*-POzi/PDMAA/clay hydrogel samples after 10 times consecutive cyclic tensile loading-unloading tests.

### The stability of POx-*b*-POzi/clay hydrogel in water:

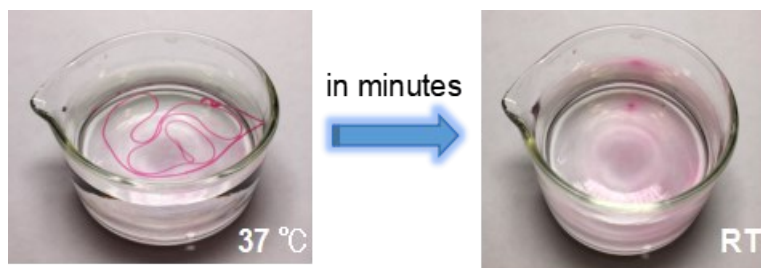


**Figure S6:** Injection of POx-*b*-POzi/clay hydrogel in 37 °C water demonstrating its fast-thermogelling property, while the formed hydrogel fiber dissolved in minutes because of the weak physical network and dilution in water (died red by carmine).

### Extrusion-based printing equipment:

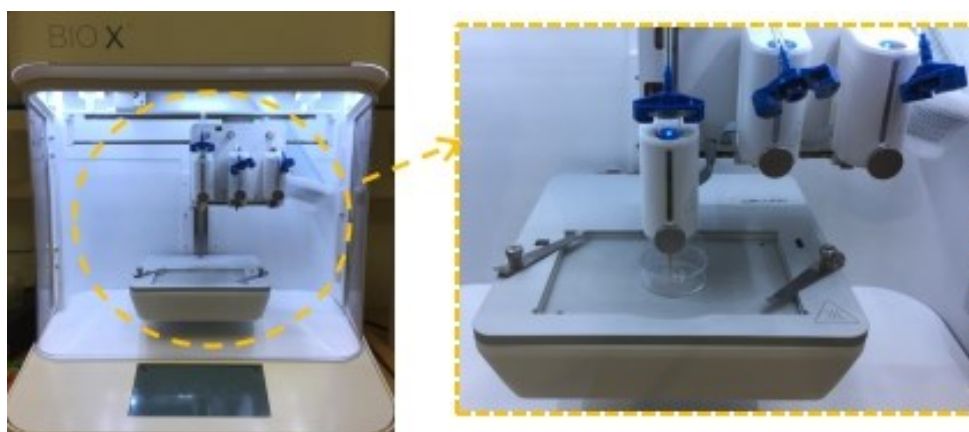


**Figure S7:** Extrusion-based printing equipment used in this work.

### 3D printing of a hollow five-pointed star, and the stability of 3D printed cube in 60 °C silicone oil:

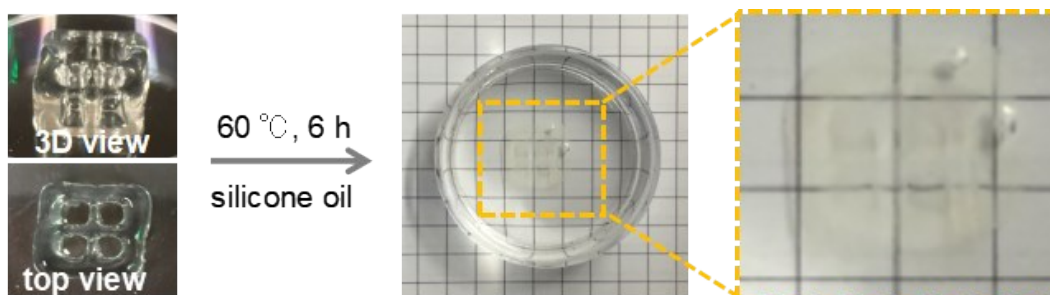


**Figure S8:** Photographs of the printed 20-layers cube (10 × 10 × 5 mm) with POx-*b*-POzi/DMAA/clay hydrogel ink, and its stability in 60 °C silicone oil.

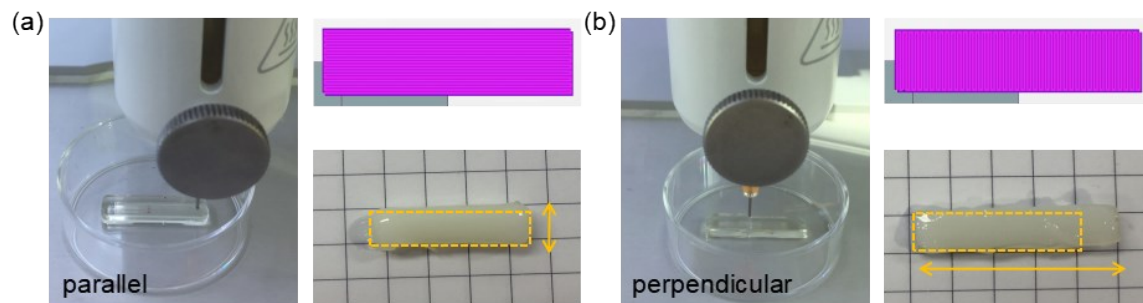


**Figure S9:** Photographs to show the 3D printing process, top view of the designed stripes ( $20 \times 5 \times 5$  mm) and printed hydrogels with parallel (a) and perpendicular (b) filament orientation to the uniaxial stretching direction. The yellow arrow indicates the merging direction, and the yellow dashed box represents the theoretical size of the hydrogel.

**Video S1:** Tensile test of POx-*b*-POzi/PDMAA/clay hydrogel (AVI)

**Video S2:** Printing of POx-*b*-POzi/DMAA/clay hydrogel precursor (AVI)